Chemical Papers
https://doi.org/10.1007/s11696-020-01280-5

ORIGINAL PAPER

An electrochemical label-free DNA impedimetric sensor with AuNP-modified glass fiber/carbonaceous electrode for the detection of HIV-1 DNA

Ece Ç. Yeter[1] · Samet Şahin[2] · M. Oguzhan Caglayan[2] · Zafer Üstündağ[1]

Received: 23 April 2020 / Accepted: 6 July 2020

Abstract
In this study, a highly sensitive, electrochemical, and label-free DNA impedimetric sensor was developed using carbonized glass fiber–coal tar pitch (GF–CTP) electrodes supported with gold nanoparticles (AuNPs) for the detection of HIV-1 gene. Thiol-modified GF–CTP electrodes were prepared using amine crosslinking chemistry and AuNPs were self-assembled obtaining highly conductive nanoelectrodes, GF–CTP–ATP–Au. All steps of electrode modifications were characterized using electrochemical, spectroscopic, and microscopic methods. GF–CTP–ATP–Au electrode was then modified with a capture DNA probe (C-ssDNA) and optimized with a target DNA probe in terms of hybridization time and temperature between 30 and 180 min and 20–50 °C, respectively. Finally, the analytic performance of the developed ssDNA biosensor was evaluated using electrochemical impedance spectroscopy. The calibration of the sensor was obtained between 0.1 pM and 10 nM analyte working range. The limit of detection was calculated using signal to noise ratio of 3 (S/N = 3) as 13 fM. Moreover, interference results for two noncomplementary DNA probes were also tested to demonstrate non-specific ssDNA interactions. An electrochemical label-free DNA impedimetric sensor was successfully developed using a novel GF–CTP–ATP–Au electrode. This study suggests that highly sensitive DNA-based biosensors can be developed using relatively low-cost carbonaceous materials.

Keywords Carbonaceous materials · Impedimetric sensor · DNA sensor · HIV-1 · Coal tar pitch

Introduction

Viruses cause many morbidities and mortalities worldwide as they can spread in many ways. The major viral pathogens include influenza virus, respiratory syncytial virus, and coronavirus that can cause acute respiratory diseases; on the other hand, some viruses attack the immune system such as human immunodeficiency virus (HIV) (Mahony 2008). World Health Organization estimates that approximately 37.9 million people were living with HIV at the end of 2018 with only 62% receiving lifelong antiretroviral therapy (WHO 2019). HIV infection, therefore, still is a major public health issue in the world; moreover, HIV testing is not accessible to everyone. There are two types of HIVs: HIV-1 and HIV-2, but research on HIV mostly focuses on HIV-1 since it is more viral and pandemic (Fatin et al. 2016).

HIV-1 can be detected using several methods. The methods used for HIV-1 detection include enzyme-linked immunosorbent assay (Re et al. 2001), western blot (Pagans et al. 2011), immunostaining (Del Valle et al. 2000), fluorescence immunoassay (Yamamoto and Kumar 2000), quartz crystal microbalance (Minunni et al. 2004), surface plasmon resonance chip (Tombelli et al. 2005), field-effect transistor (Ruslinda et al. 2013) and biosensors (Laksanasopin et al. 2015). Most of these methods rely on antibody–antigen reaction and it provides accurate results; however, it is time-consuming and costly as well as requires large sample volumes. On the other hand, electrochemical biosensors can be a good alternative due to their simplicity, relatively low cost, high sensitivity, and their potential for point of care use.

✉ Samet Şahin
samet.sahin@bilecik.edu.tr

✉ Zafer Üstündağ
zustundag@gmail.com

[1] Department of Chemistry, Kütahya Dumlupınar University, 43100 Kütahya, Turkey

[2] Department of Bioengineering, Bilecik Şeyh Edebali University, 11230 Bilecik, Turkey

Published online: 13 July 2020

Various electrochemical methods have been developed for the detection of the HIV-1 gene recently. Square wave voltammetry (Zhang et al. 2010), differential pulse voltammetry (Li et al. 2014), amperometry (Gao et al. 2018), electrogenerated chemiluminescence (Poorghasem et al. 2016) and electrochemical impedance spectroscopy (EIS) (Gong et al. 2015) techniques were employed to design ultra-sensitive HIV-1 DNA biosensors. Most of them resulted in a limit of detection values of below pM concentrations for pM–nM detection ranges. However, some of the mentioned methods require hybridization indicators or redox-labels that bring complexity to sensor design; therefore, a label-free electrochemical biosensor would be desirable. EIS, on the other hand, can produce ultra-sensitive results without the need of a redox or any other labeling for hybridization and electrochemical signal production. Promising results for the detection of HIV-1 gene have been obtained using EIS reaching pM to fM concentrations (Gong et al. 2017). Recently, electrochemical studies based on EIS and differential pulse voltammetry (DPV) have been reported with a limit of detection values of as low as 8.3 fM utilizing carbon nanostructures (Jia et al. 2019; Li et al. 2020). However, the cost and complex synthesis processes of nanostructures such as carbon nanotubes (CNTs) and graphene are still a concern. Therefore, more efficient and low-cost ways to produce electrically conductive electrodes are essential for sensor development.

Carbonaceous materials (CMs) such as CNTs and graphene have attracted so many researchers for the last 2 decades (Jana et al. 2013). CMs show excellent mechanical properties and electrical conductivity which make them a perfect candidate for industrial applications such as solar cells (Chen et al. 2014), hydrogen storage (Hassan et al. 2007), supercapacitors (Frackowiak et al. 2006) and sensors (Wei et al. 2013). However, CNTs and GPH are some of the expensive examples of CMs; on the other hand, low-cost CMs can also be synthesized using low-cost alternatives such as coal tar pitch (CTP). Carbonized CTP can be a very good alternative with high surface area and excellent electrical conductivity especially for the synthesis of CTP composites (Erkal et al. 2016). GF is a low-cost and commercially available material often used in refractor materials and furnace insulations due to aluminum silicate in the structure; therefore, its use in bioelectronic applications is limited. However, when carbonized with CTP, its electrical properties could dramatically improve.

DNA immobilization and hybridization efficiencies are very important to construct ultra-sensitive biosensors; therefore, several nanomaterials such as gold nanoparticles (AuNPs) (Cai et al. 2001), ZnO (Yumak et al. 2011), Fe/Pt/ZSn nanocore–shell (Chang and Wu 2010), a mercaptoaceticacid-modified cadmium sulfide (Sun et al. 2007), and carbon-nanotubes/nanozirconiumdioxide/chitosan (Yang et al. 2007) have been used to help DNA immobilization and hybridization. Among all, AuNPs are the most employed nanomaterial and previous results showed that both immobilization and hybridization qualities are improved using AuNP-supported electrodes compare to their bare form.

In this work, a novel material based on glass fiber (GF) was first developed using CTP, and then a highly sensitive, electrochemical, and label-free DNA impedimetric sensor was developed using carbonized GF–CTP electrodes supported with AuNPs for the detection of the HIV-1 DNA. Different electrode conformations were prepared for electrochemical and surface characterizations. Voltammetric and impedimetric analyses were used for electrochemical characterization; IR spectroscopy, scanning electron microscopy–energy-dispersive X-ray spectroscopy (SEM–EDX), X-ray photoelectron spectroscopy (XPS), and transmission electron microscopy (TEM) analyses were used for the characterization of the electrodes. The analytic performance of the developed DNA biosensor was evaluated using EIS. This study, to the best of authors' knowledge, is a pioneer demonstration of the carbonization of GF with CTP for sensor applications. Therefore, highly sensitive DNA-based biosensors can be developed using relatively low-cost carbon materials, and more sensitive results can be achieved with further modifications.

Experimental

Materials

Tetrachloroauric (III) acid (Sigma-Aldrich, 99%), trisodium citrate (Merck, > 99%), 1-ethyl-3-(3-dimethylaminopropyl) carbodiimide (EDC, Sigma-Aldrich), *N*-hydroxysuccinimide (NHS, Sigma-Aldrich), 4-aminothiophenol (ATP, Sigma-Aldrich), acetonitrile (Riedel, HPLC grade), ethanol (Merck, absolute), $K_3Fe(CN)_6/K_4Fe(CN)_6$ (Sigma-Aldrich, > 99.9%), DNA probes (Helix Bio), CTP (Orcan Company) and other chemicals of reagent grade were used as received from the supplier. All reagents and standards were prepared in ultrapure water (UPW, Human Power 1 + , Korea). The electrochemical experiments were carried out with an Ivium CompactStat (NL). The electrochemical measurements were performed using a three-electrode system under high-purity argon (99.999%) atmosphere at room temperature (24 ± 1 °C). The reference electrode was an Ag/AgCl (Sat) electrode, the auxiliary electrode a platinum wire. AuNP-modified glass fiber/carbonaceous disk electrode was used as a working electrode. The electrode surface area was adjusted as 0.071 cm^2 with an O-ring in the Teflon tube.

Preparation of thiol-modified carbon disk electrodes

The preparation of carbonized sensor materials and its sensor application was performed accordingly to the procedure described in E. C. Yeter's M.Sc. thesis (Yeter 2018). Thiol (SH-)-terminated CTP-coated glass fiber (GF) electrodes were prepared according to the procedure described elsewhere (Güzel et al. 2010) using amine cross-linking chemistry. Briefly, GF was washed with UPW, ethanol, and acetonitrile, respectively, for 10 min in an ultrasonic bath. 10 g of dried GF was then mixed and homogenized with 10 g of CTP in acetone. Carbonization of the GF–CTP mixture was carried out in a tube furnace (Protherm, USA) at 1000 °C with a heating rate of 10 °C/min at under nitrogen atmosphere. Carbonized GF–CTP was ground into fine powder in a planetary ball mill (Retcsch/PM100, Germany) for 1 h under 500 rpm. Disk electrodes were prepared under pressure using a 'kamalak' (*Cedrus libani A. Rich.*) resin in ethanol as a binder with GF–CTP and CTP (Üstündağ and Erkal 2017).

GF–CTP electrodes were then prepared for AuNP modification.

The schematic representation of the modification process for AuNP terminated carbonaceous material is shown in Fig. 1. First, GF–CTP was treated with 4 M HNO_3 for 12 h to obtain carboxylic acid groups on the surface (denoted as GF–CTP–COOH). GF–CTP–COOH was then washed with UPW and COOH groups were activated with 0.01 M EDC and NHS mixture in 0.1 M potassium phosphate buffered solution (PBS) at pH 7 for 12 h. Activated COOH groups were modified with 1 mM ATP, 0.1 M PBS, pH 7, for 8 h and denoted as GF–CTP–ATP.

Preparation of gold nanoparticles (AuNPs) and AuNP-modified carbonaceous disk electrodes

250 µL of tetrachloroauric (III) acid (25 mM, $HAuCl_4.3H_2O$) solution was first diluted to 50 mL, and 5 mL of 1.5% trisodium citrate solution was slowly added under 500 rpm vigorous stirring at 98 °C. Upon color change to wine red, the colloidal solution was cooled down to 4 °C and centrifuged (Hermle, Z36HK, Germany) at 20,000 rpm. The obtained AuNPs were then washed twice with UPW and absolute ethanol, respectively, and kept at 4 °C in ethanol when not in use. GF–CTP–ATP electrodes were then immersed in an ethanoic AuNP solution for 8 h to obtain self-assembled monolayers (SAMs) on the electrode surface. Final electrode conformation was denoted as GF–CTP–ATP—ATP–Au.

Characterization of the carbonaceous electrodes

GF–CTP–ATP—ATP–Au, GF–CTP–ATP, GF–CTP, CTP, and glassy carbon (GC) electrodes were first characterized using linear sweep voltammetry (LSV) and electrochemical impedance spectroscopy (EIS). All tested electrodes have a

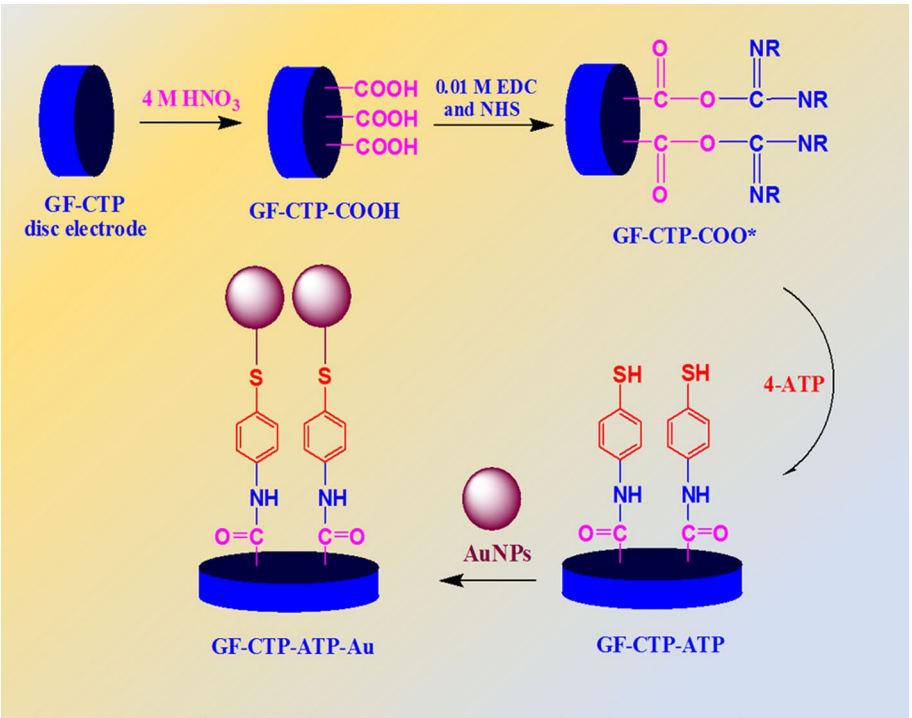

Fig. 1 Schematic diagram of the AuNP modification on GF–CTP electrode

surface area of 0.071 cm^2 and all electrochemical tests were performed using 2 mM $K_3Fe(CN)_6/K_4Fe(CN)_6$ redox probe in 0.1 M KCl. IR spectroscopy (Bruker, Tensor-27, Germany), SEM–EDX (Nova, NanoSEM-650, Belgium), XPS (PHI 5000-Versa Probe, Φ ULVAC-PHI.Inc., Japan/USA) and TEM (JEOL Ltd., Tokyo, Japan) analyses were used for the characterization of the prepared electrodes and AuNPs.

ssDNA-based impedimetric sensor characterization

Table 1 shows a summary of the single-strand DNA (ssDNA) oligonucleotides used in this study. All ssDNA oligonucleotide solutions were prepared using 20 mM NaCl at pH 7.4 and kept at − 20 °C when not in use.

GF–CTP–ATP–Au electrode surface was first modified with 1 µM of C-ssDNA (Ella Biotech GmbH, Germany) for 1 h following by a washing step with UPW to remove unbound C-ssDNA molecules. This conformation was denoted as GF–CTP–ATP–Au/C-ssDNA. Optimization of the ss-DNA-based impedimetric sensor was performed using EIS in 2 mM $K_3Fe(CN)_6/K_4Fe(CN)_6$ redox couple (0.1 M KCl) for hybridization time and temperature parameters. Hybridization time is defined as the interaction time between C-ssDNA and T-ssDNA. Hybridization time and temperature ranges were chosen as 30–180 min and 20–50 °C, respectively. The sensor calibration range was chosen as 0.1 pM – 10 nM. The schematic representation of the detecting principle for T-ssDNA is given in Fig. 2. The stability of the sensor was calculated using 1 nM T-ssDNA and accuracy tests were conducted using 100 pM and 1 nM T-ssDNA for 7 days. Finally, selectivity was determined using two different ss-DNA strands for 10 nM T-ssDNA.

Results and discussion

To evaluate the effect of the modifications performed on disk electrode surfaces, LSV and EIS tests were first conducted. Figure 3a shows that the GF–CTP–ATP–Au electrode has the highest oxidation peak potential reaching around ca. 30 µA current response indicating enhanced signal response compared to CTP electrode and commercial GC electrode. This behavior was further confirmed using EIS technique (frequency range from 100 to 0.1 kHz with 10 mV wave amplitude at a DC potential of 0.115 V in 2 mM $K_3Fe(CN)_6/K_4Fe(CN)_6$ redox probe in 0.1 M KCl) and the Nyquist plots of the redox couple for each electrode are shown in Fig. 3b.

Charge transfer resistance (R_{ct}) values were calculated for each electrode by fitting the EIS data using a Warburg-effected diffusion-controlled type equivalent circuit (Randviir and Banks 2013). A sample equivalent circuit and fitted experimental data can be seen from Fig. 3c. The R_{ct} values for GC, CTP, GF–CTP, GF–CTP–ATP, and GF–CTP–ATP–Au were calculated as 9.41 ± 0.67, 8.83 ± 0.74, 6.44 ± 0.47, 5.57 ± 0.41, and 1.83 ± 0.17 kΩ, respectively. Impedance analysis showed that GF–CTP–ATP–Au electrode has the lowest charge transfer resistance indicating fast electron transfer type kinetics for the redox probes compared to other tested electrodes. Voltammetry and impedance tests, therefore, confirmed that AuNPs enhanced the electron transfer rate of redox probes providing minimum charge transfer resistance among prepared electrodes.

Figure 3d shows the stability of the GF–CTP–ATP–Au electrode when kept in open-air conditions at room temperature for 10 days. The oxidation peak current for 2 mM $K_3Fe(CN)_6/K_4Fe(CN)_6$ redox probe was changed from 30.33 ± 0.35 µA to 30.27 ± 0.41 µA showing that the GF–CTP–ATP–Au electrode has very good stability. This superior electrochemical properties and good stability of GF–CTP–ATP–Au could be due to the tunneling effect of the nanoparticle-supported carbonaceous structure (Sayed et al. 2012).

Figure 4 also shows SEM and EDX analyses of the GF electrode before and after carbonization. Figure 4a, b does not show distinctive differences between GF and GF–CTP; however, the EDX spectrum (Fig. 4c) confirms that GF is coated with CTP confirmed with the appearance of C (Kα1). Furthermore, EDX results revealed that no C was found in GF; on the other hand, GF–CTP electrode has 2% C by weight.

Figure 5a shows the TEM image of synthesized AuNP confirming 10–60 nm size spherical-like AuNPs was successfully synthesized. IR analysis of GF–CTP–ATP (Fig. 5b) shows that GF has its characteristic peaks at 950–1500 cm^{-1} and 550–800 cm^{-1} for Al–O–Si deformation and Si–O

Table 1 Summary of the DNA oligonucleotides used in this study

ssDNA	ssDNA Sequence
Capture ssDNA (C-ssDNA)	5′-HS-$(CH_2)_4$-GATCGCCCTTTTCCATTTCCATAC ATATTTCTGTTA-3’
Target ssDNA (T-ssDNA)	3′-GGAAAAGGTAAAGGTATGTATAAAGACAAT-5’
Non-specific ssDNA-1 (NC1-ssDNA)	3′-ATAATCCACCTATCCCAGTAGGAGAAAT-5’
Non-specific DNA-2 (NC2-ssDNA)	3′-TTAGCTCGTATAGCCGCTACCTAGGGAT-5’

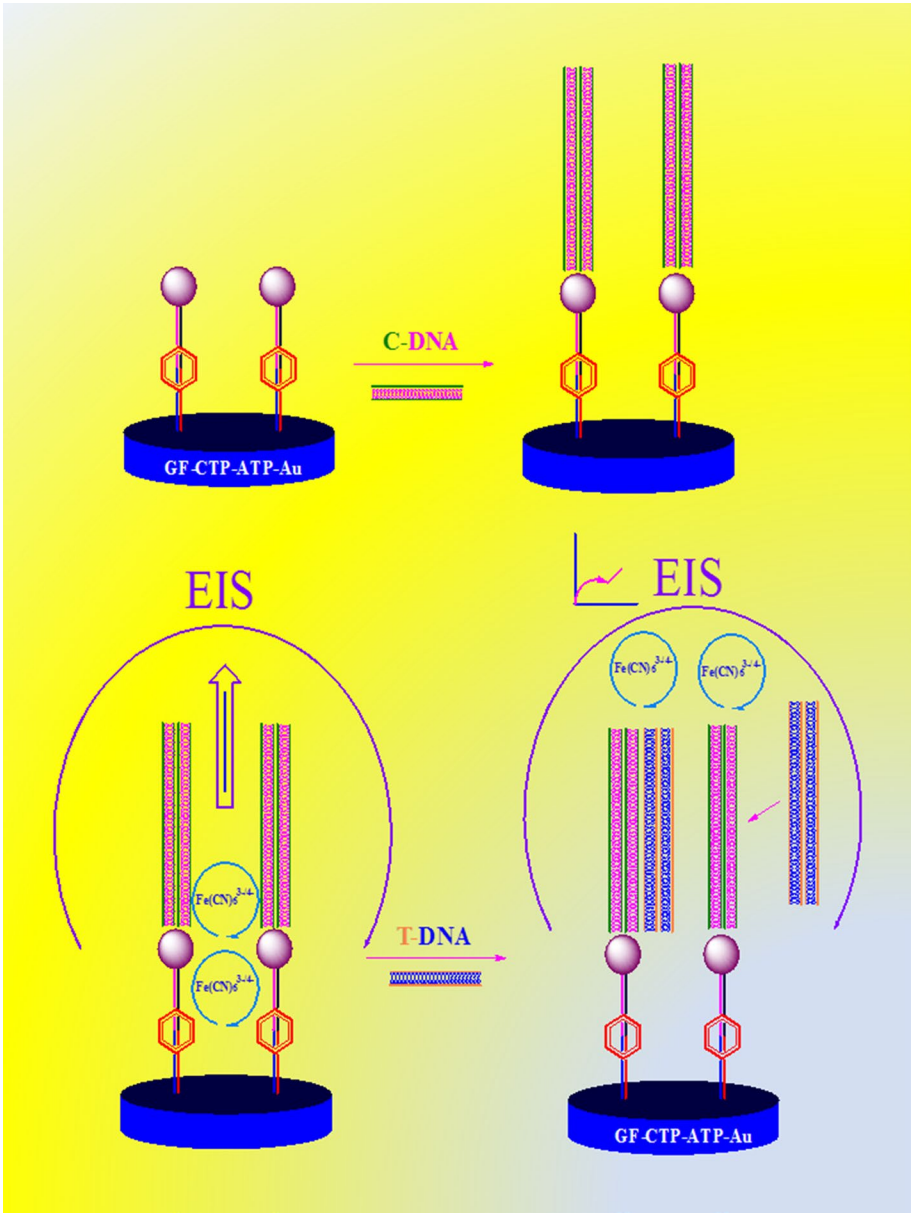

Fig. 2 Schematic diagram of the detecting principle for T-ssDNA

quartz, respectively. Moreover, Si–O–Si and H–O–H conformations can also be seen at 475 cm^{-1} and 1650 cm^{-1}, respectively (Rondón et al. 2013; Vaculikova et al. 2011). After the carbonization process (GF–CTP), we can observe aliphatic and aromatic C–H interactions at 2700–3000 cm^{-1} and 3000–3100 cm^{-1}, respectively. O–H stretching was seen at 3000–3500 cm^{-1} after the carbonization process. Besides, aromatic C–H bending can be seen between 650 and 1000 cm^{-1}. Aromatic ring mode can also be seen around 1600 cm^{-1}. Finally, upon amine functionalization, -C = O (carbonyl) peaks appeared at 1720 cm^{-1} and N–H groups can be seen at 3400–3700 cm^{-1} (Cheng et al. 2014; Çelik et al. 2016; Lin et al. 2005).

High-resolution narrow spectra of GF–CTP–ATP–Au electrode for C_{1s}, N_{1s}, $S_{2p,}$ and Au_{4f} are given in Fig. 6. High-resolution C1s narrow spectrum of the GF–CTP–ATP–Au electrode is given in Fig. 6a. When the C_{1s} region is fitted, three main peaks regarding -COO, -C = O and -CH were obtained at 288.6 eV, 285.6 eV, and 283.5 eV, respectively. Similarly, N_{1s} binding energy was obtained at 400.8 eV. Furthermore, $S_{2p}{}^{1/2}$ and $S_{2p}{}^{3/2}$ binding energies were obtained at 167.8 eV and 162.7 eV respectively. Finally, $Au_{4f}{}^{5/2}$ and $Au_{4f}{}^{7/2}$ binding energies were obtained at 87.5 eV and 83.9 eV, respectively. As a result, XPS analysis confirmed the formation of a carbonaceous electrode with ATP amidization and the functionalization of AuNPs on -SH groups.

Optimization studies were carried out to confirm the hybridization time and temperature for GF–CTP–ATP–Au. First, the electrode was modified with C-ssDNA for 1 h

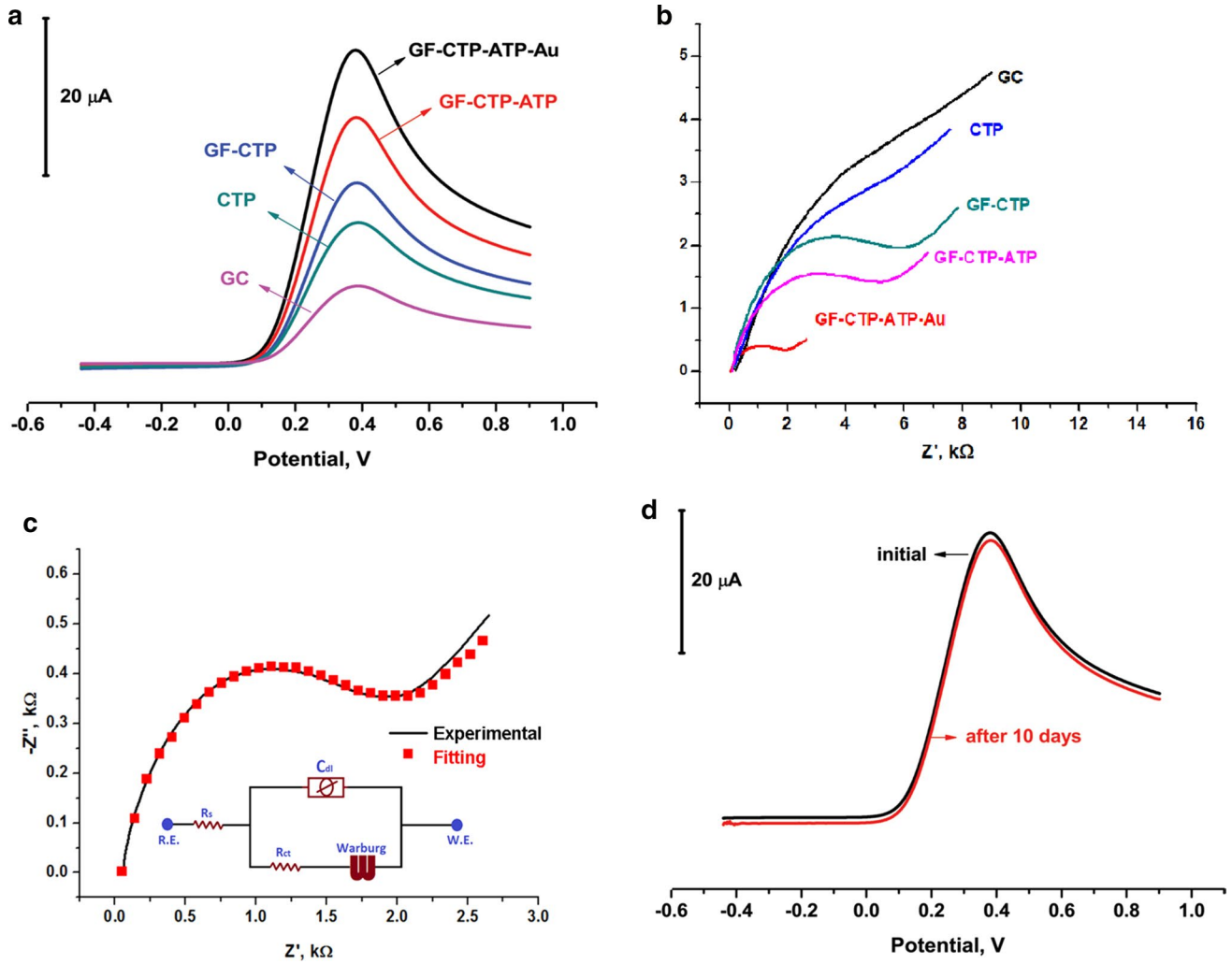

Fig. 3 **a** LSV scans and **b** Nyquist plots of different electrode conformations in 2 mM $K_3Fe(CN)_6/K_4Fe(CN)_6$ redox probe (in 0.1 M KCl). **c** Equivalent circuit and fitted experimental data for GF–CTP–ATP–Au electrode. **d** Stability of the GF–CTP–ATP–Au electrode when kept in open-air conditions at room temperature for 10 days, tested in 2 mM $K_3Fe(CN)_6/K_4Fe(CN)_6$ redox probe (in 0.1 M KCl)

and washed excessively with UPW to remove unbounded ssDNA. GF–CTP–ATP–Au/C-ssDNA was then exposed to 10 nM T-ssDNA for 30 to 180 min from 20 to 50 ºC. Figure 7 shows the optimization results for (1) hybridization time and (2) temperature using R_{ct} data obtained from EIS analysis. Figure 7 shows that hybridization time and the temperature reached a plateau at 90 min and 35 ºC, respectively. Therefore, these parameters were used to obtain calibration curves for the ssDNA sensor.

The calibration of the ssDNA sensor was obtained using the EIS technique between 0.1 pM and 10 nM analyte working range. Figure 8 shows the Nyquist data and calibration curve for the developed ssDNA sensor. It can be seen that the R_{ct} values increased upon the increasing concentration of T-ssDNA indicating that the electron transfer rate of the redox couple becomes dramatically limited. This type of behavior from DNA hybridization in impedance analysis can also be seen from similar studies in the literature (Bonanni and Pumera 2011; Riedel et al. 2014). The limit of detection (LOD) was calculated using a signal to noise ratio of 3 (S/N = 3) as 13 fM. This is one of the highest LOD values with a wide range of detection range among various DNA-based sensors (Gupta et al. 2013; Liu et al. 2010; Yang et al. 2012; Zhang et al. 2011; Zhu et al. 2005).

The stability of the prepared C-ssDNA sensor for T-ssDNA hybridization is presented in Table 2 for 7-day tests. The prepared sensor showed very good stability over 7 days changing between 96.7% and 101.4% for minimum and maximum obtained recoveries, respectively. When considered for 95% confidence level, the obtained stability results do not show a significant difference during 7 days.

Precision (RSD %) and accuracy measurements were conducted for two different concentrations of T-ssDNA (100 pM and 1 nM). Experiments were performed in two

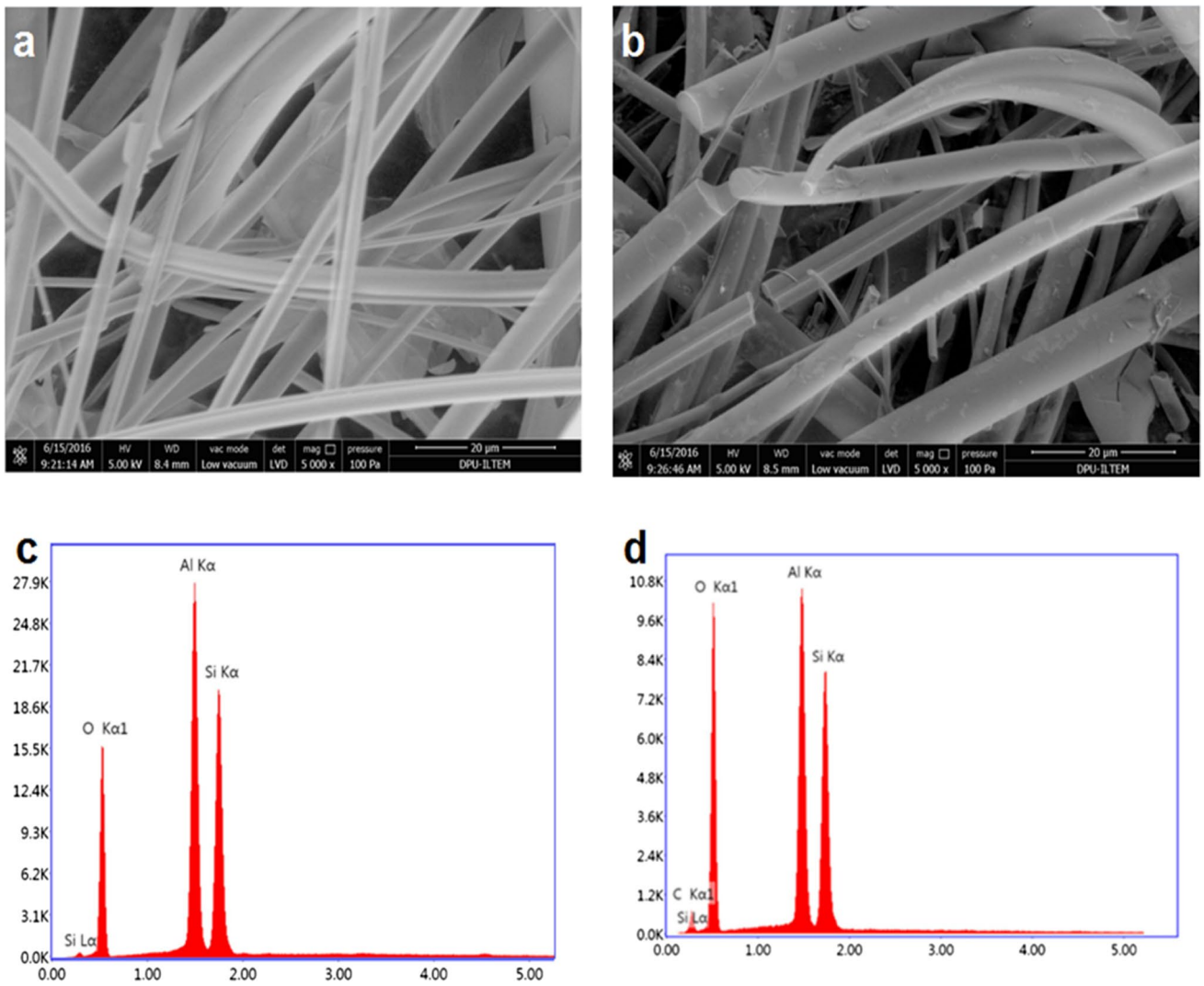

Fig. 4 SEM imaging of **a** GF and **b** GF–CTP and EDX spectra of **c** GF and **d** GF–CTP

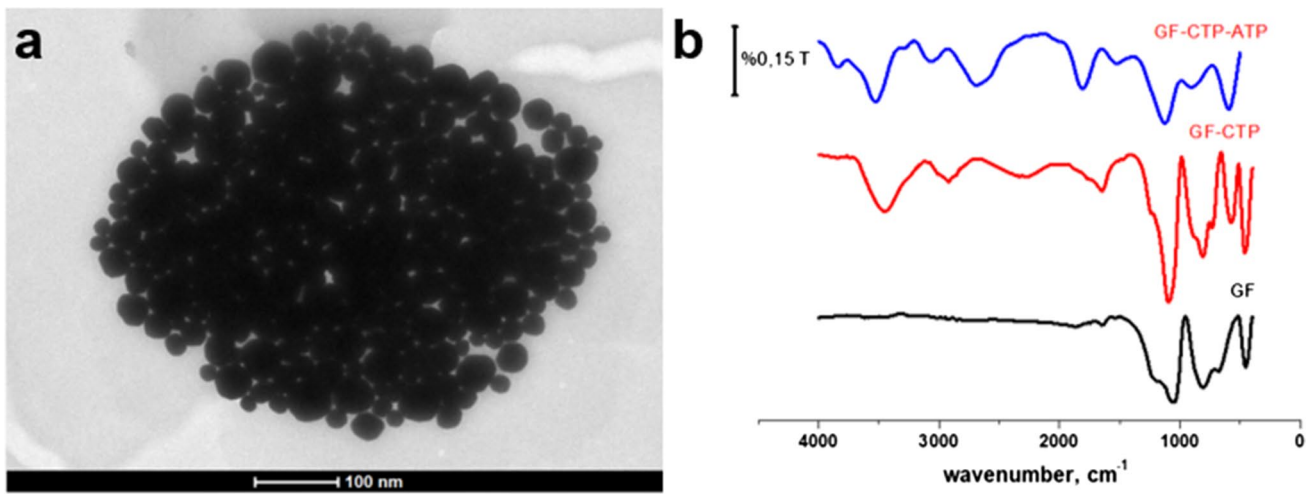

Fig. 5 **a** TEM images of synthesized AuNPs and **b** IR spectra of GF, GF–CTP and GF–CTP–ATP electrodes

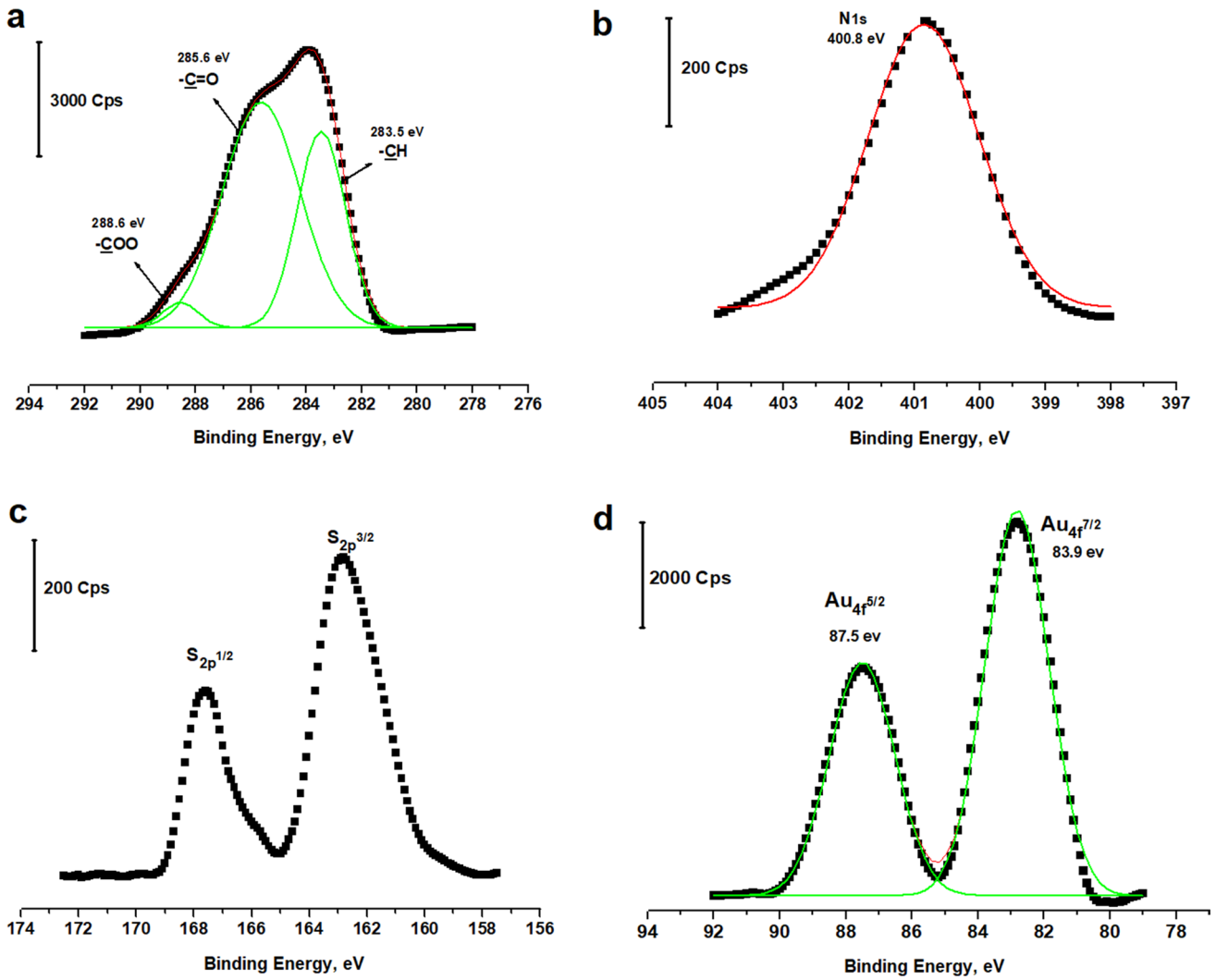

Fig. 6 XPS narrow spectra of **a** C_{1s}, **b** N_{1s}, **c** S_{2p}, **d** Au_{4f}

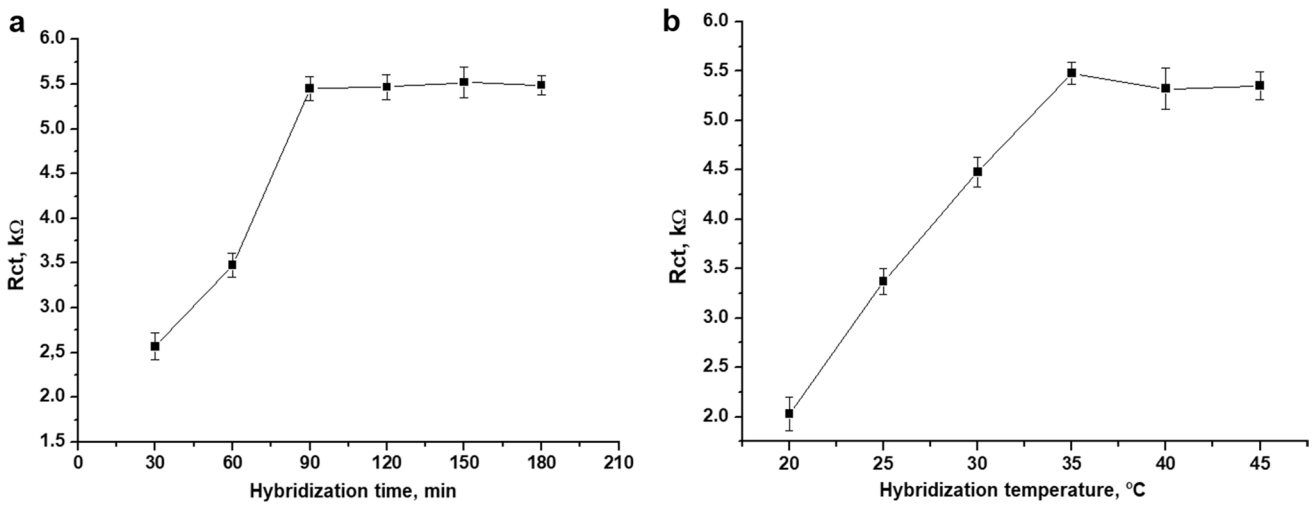

Fig. 7 Optimization of **a** hybridization time and **b** temperature for GF–CTP–ATP–Au/C-ssDNA after exposed to 10 nM T-ssDNA, tested in 2 mM $K_3Fe(CN)_6/K_4Fe(CN)_6$ redox probe (in 0.1 M KCl). Hybridization time tests were conducted at 35 ºC. Error bars are sample standard deviations ($N = 5$ samples)

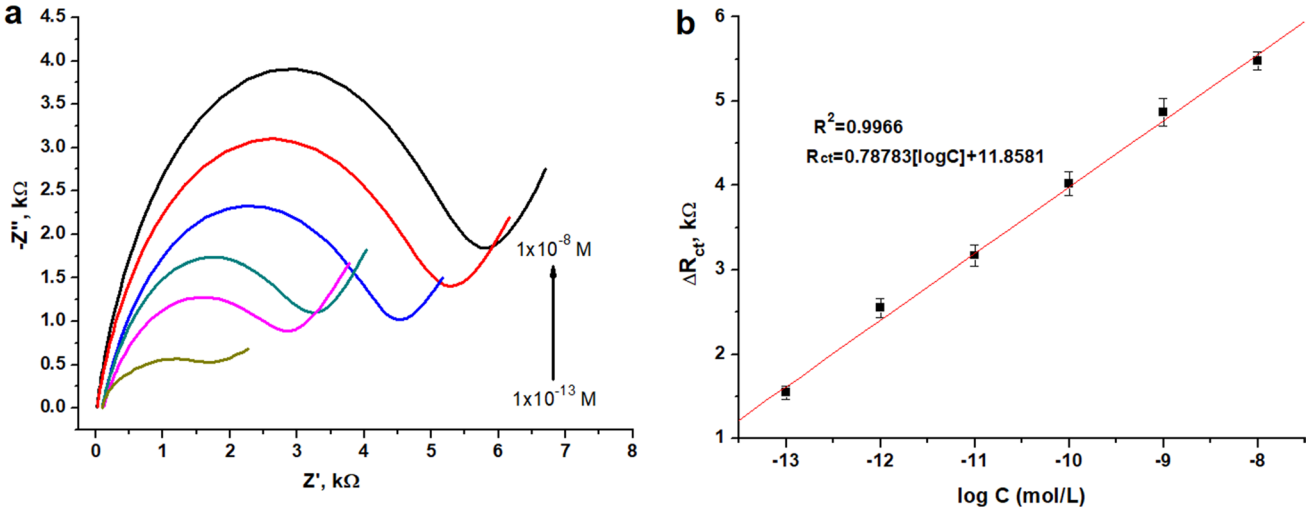

Fig. 8 The Nyquist data and **b** calibration curve for the developed ssDNA sensor. Error bars are sample standard deviations ($N = 5$ samples)

Table 2 Stability of the ssDNA sensor for T-ssDNA hybridization. Error bars are sample standard deviations ($N = 5$ samples)

Day	R_{ct}, kΩ	RSD %
1	4.87 ± 0.6	–
2	4.79 ± 0.11	98.4
3	4.85 ± 0.15	99.6
4	4.71 ± 0.15	96.7
5	4.94 ± 0.11	101.4
6	4.83 ± 0.17	99.2
7	4.80 ± 0.16	98.6

Table 3 Precision and accuracy of the ssDNA sensor

Found value		Added T-DNA	
		100.0 pM	1.00 nM
Intra-day	Found value	98.6 ± 2.18	1.02 ± 0.01
	RSD %	2.211	0.980
	Accuracy %	− 1.4	2.0
Inter-day	Found value	99.16 ± 1.74	0.98 ± 0.01
	RSD %	1.755	1.020
	Accuracy %	− 0.84	− 2.0

Error bars are sample standard deviations ($N = 5$ samples)

different modes: intra-day and inter-day precision for five independent samples. Moreover, inter-day precision measurements were performed for seven consecutive days. The obtained results are given in Table 3. RSD % and accuracy results show that the proposed method provides RSD % and accuracy % values not more than around ≤ 2.2% and ≥ − 2%, respectively, for both intra-day and inter-day measurements. This indicates very good precision and accuracy for the developed ssDNA sensor.

Table 4 The effect of possible interfering ssDNAs on the sensor

Interfering ssDNA	Concentration, (μM)	R_{ct} change %
NC_1-DNA	1.0	− 1.24
NC_2-DNA	1.0	0.96

Table 4 shows the interference results for two possible interferences, NC_1-ssDNA and NC_2-ssDNA to test non-specific ssDNA interactions. It can be seen from Table 4 that the change in the value of R_{ct} is negligible compared to the values obtained for the T-ssDNA for the interfering ssDNAs. Therefore, no specific interaction from the selected ssDNAs was observed.

The proposed ssDNA sensor shows a lower LOD with a broad detection range for HIV-1 DNA detection than recently published studies using EIS (Table 5). This is mainly because of the highly conductive carbon fiber structures obtained after the carbonization process and the contribution of Au on the electrode surface. Moreover, the carbon fiber structure also provides a very high active surface area. DPV and amperometry are other electrochemical methods that provide a range of limits of detection values among which a recent study based on DPV performs similar to this study. The main advantages of this work are that (1) a low-cost raw material (GF) was converted into valuable conducting electrode material (GF–CTP) and (2) its performance was further improved using a simple approach. As a result, a highly sensitive impedimetric ssDNA sensor for HIV-1 DNA was successfully developed.

Table 5 Analytical performance of some of the recent studies in the literature based on electrochemical HIV DNA detection

Electrode	Technique	Linear range	LOD	References
hpDNA/Au	Amperometry	10 pM–50 nM	150 fM	(Gao et al. 2018)
NH_2-rGO/beta-CD/GCE	DPV	0.05 pM–1 pM	8.7 fM	(Li et al. 2020)
$NiCo_2O_4$/CoO@CNTs	EIS	0.1 pM–20 nM	16.7 fM	(Jia et al. 2019)
GN/Nafion/GCE	EIS	0.1 pM –100 nM	23 fM	(Gong et al. 2017)
GF–CTP–ATP–Au/C-ssDNA	EIS	0.1 pM–10 nM	13 fM	This work

Conclusions

A novel and sensitive carbonaceous electrode was designed for HIV-1 detection using a label-free DNA probe. A low-cost and commercially available GF is utilized to obtain highly conductive and high-surface area electrode material due to its fiber structure and carbonization process. Moreover, this structure was further improved using self-ordered AuNPs attached to the thiol-modified GF–CTP electrode. Electrochemical investigations showed successful attachment of each modification layer on electrodes. XPS and IR results also confirmed the structure of the Au-attached carbonized electrode. Optimization studies revealed that hybridization time and temperature of C-ssDNA and T-ssDNA were stable after 90 min and 35 ºC, respectively. The calibration of the sensor was obtained using EIS between 0.1 pM and 10 nM (1×10^{-13} and 1×10^{-8} M) with 13 fM (1.3×10^{-14}M) detection limit. No significant non-specific ssDNA interactions were observed for two different noncomplementary DNA probes chosen. Furthermore, very good precision and accuracy for the ssDNA sensor were obtained providing RSD % and accuracy % values between 2.2% and − 2%, respectively, for both intra-day and inter-day measurements. This study shows one of the best analytic performance parameters compared to similar ssDNA-based sensors in the literature providing a low-cost and easy electrode preparation methodology that could also be used in different analyte-sensing strategies.

Compliance with ethical standards

Conflict of interest On behalf of all authors, the corresponding authors state that there is no conflictof interest.

References

Bonanni A, Pumera M (2011) Graphene platform for hairpin-DNA-based impedimetric genosensing. ACS Nano 5:2356–2361. https://doi.org/10.1021/nn200091p

Cai H, Xu C, He P, Fang Y (2001) Colloid Au-enhanced DNA immobilization for the electrochemical detection of sequence-specific DNA. J Electroanal Chem 510(78):85

Chang H, Wu S-h (2010) Hybridization of FePt/ZnS nanocore-shell structure with DNAs of different sequences. Mater Trans 51:2094–2098

Chen J-G, Vittal R, Yeh M-H, Chen C-Y, Wu C-G, Ho K-C (2014) Carbonaceous allotropes modified ionic liquid electrolytes for efficient quasi-solid-state dye-sensitized solar cells. Electrochim Acta 130:587–593

Cheng Y, Fang C, Su J, Yu R, Li T (2014) Carbonization behavior and mesophase conversion kinetics of coal tar pitch using a low temperature molten salt method. J Anal Appl Pyrol 109:90–97

Çelik GK, Üzdürmez AF, Erkal A, Kılıç E, Solak AO, Üstündağ Z (2016) 3, 8-Diaminobenzo [c] cinnoline derivatived graphene oxide modified graphene oxide sensor for the voltammetric determination of Cd 2+ and Pb 2+. Electrocatalysis 7:207–214

Del Valle L, Croul S, Morgello S, Amini S, Rappaport J, Khalili K (2000) Detection of HIV-1 Tat and JCV capsid protein, VP1, in AIDS brain with progressive multifocal leukoencephalopathy. J Neurovirol 6:221–228

Erkal A, Aşık İ, Yavuz S, Kariper A, Üstündağ Z (2016) Biosensor application of carbonaceous nanocoil material: preparation, characterization, and determination of dopamine and uric acid in the presence of ascorbic acid. J Electrochem Soc 163:H269–H277

Fatin M et al (2016) HIV-1 Tat biosensor: current development and trends for early detection strategies. Biosens Bioelect 78:358–366

Frackowiak E, Machnikowski J, Béguin F (2006) Novel carbonaceous materials for application in the electrochemical supercapacitors. In: new carbon based materials for electrochemical energy storage systems: Batteries, Supercapacitors and Fuel Cells. Springer, pp 5–20

Gao X, Wang X, Li Y, He J, Yu H-Z (2018) Exonuclease I-hydrolysis assisted electrochemical quantitation of surface-immobilized DNA hairpins and improved HIV-1 gene detection. Anal Chem 90:8147–8153

Gong Q, Wang Y, Yang H (2017) A sensitive impedimetric DNA biosensor for the determination of the HIV gene based on graphene-Nafion composite film. Biosens Bioelectron 89:565–569

Gong Q, Yang H, Dong Y, Zhang W (2015) A sensitive impedimetric DNA biosensor for the determination of the HIV gene based on electrochemically reduced graphene oxide. Anal Methods 7:2554–2562

Gupta VK, Yola ML, Qureshi MS, Solak AO, Atar N, Üstündağ Z (2013) A novel impedimetric biosensor based on graphene oxide/gold nanoplatform for detection of DNA arrays. Sens Actuators B Chem 188:1201–1211

Güzel R et al (2010) Effect of Au and Au@ Ag core–shell nanoparticles on the SERS of bridging organic molecules. J Coll Inter Sci 351:35–42

Hassan NHA, Mohamed AR, Zein SHS (2007) Study of hydrogen storage by carbonaceous material at room temperature. Diam Relat Mat 16:1517–1523

Jana P, Fierro V, Celzard A (2013) Ultralow cost reticulated carbon foams from household cleaning pad wastes. Carbon 62:517–520

Jia Z et al (2019) NiCo2O4 spinel embedded with carbon nanotubes derived from bimetallic NiCo metal-organic framework for the

ultrasensitive detection of human immune deficiency virus-1 gene. Biosens Bioelect 133:55–63
Laksanasopin T et al (2015) A smartphone dongle for diagnosis of infectious diseases at the point of care. Sci Trans Med 7:273–re271
Li B et al (2014) Sensitive HIV-1 detection in a homogeneous solution based on an electrochemical molecular beacon coupled with a nafion–graphene composite film modified screen-printed carbon electrode. Biosens Bioelectron 52:330–336
Li J, Jin X, Feng M, Huang S, Feng J (2020) Ultrasensitive and highly selective electrochemical biosensor for hiv gene detection based on amino-reduced graphene oxide and β-cyclodextrin modified glassy carbon electrode. Int J Electrochem Sci 15:2727–2738
Lin Q, Li T, Ji Y, Wang W, Wang X (2005) Study of the modification of coal-tar pitch with p-methyl benzaldehyde. Fuel 84:177–182
Liu S, Liu J, Wang L, Zhao F (2010) Development of electrochemical DNA biosensor based on gold nanoparticle modified electrode by electroless deposition. Bioelectrochemistry 79:37–42
Mahony JB (2008) Detection of respiratory viruses by molecular methods. Clin Microbiol Rev 21:716–747
Minunni M, Tombelli S, Gullotto A, Luzi E, Mascini M (2004) Development of biosensors with aptamers as bio-recognition element: the case of HIV-1 Tat protein. Biosens Bioelect 20:1149–1156
Pagans S, Sakane N, Schnölzer M, Ott M (2011) Characterization of HIV Tat modifications using novel methyl-lysine-specific antibodies. Methods 53:91–96
Poorghasem R, Saberi RS, Shayan M, Mehrgardi MA, Kiani A (2016) Closed bipolar electrochemistry for the detection of human immunodeficiency virus short oligonucleotide. Electrochim Acta 222:1483–1490
Randviir EP, Banks CE (2013) Electrochemical impedance spectroscopy: an overview of bioanalytical applications. Anal Methods 5:1098–1115
Re M, Vignoli M, Furlini G, Gibellini D, Colangeli V, Vitone F, La Placa M (2001) Antibodies against full-length Tat protein and some low-molecular-weight Tat-peptides correlate with low or undetectable viral load in HIV-1 seropositive patients. J Clin Virol 21:81–89
Riedel M, Kartchemnik J, Schöning MJ, Lisdat F (2014) Impedimetric DNA detection-steps forward to sensorial application Anal Chem 86:7867–7874
Rondón W, Freire D, Benzo Z, Sifontes A, González Y, Valero M, Brito J (2013) Application of 3A zeolite prepared from venezuelan kaolin for removal of Pb (II) from wastewater and its determination by flame atomic absorption spectrometry. Am J Anal Chem 4(10):584-593. https://doi.org/10.4236/ajac.2013.410069
Ruslinda AR, Tanabe K, Ibori S, Wang X, Kawarada H (2013) Effects of diamond-FET-based RNA aptamer sensing for detection of real sample of HIV-1 Tat protein. Biosens Bioelect 40:277–282
Sayed SY, Fereiro JA, Yan H, McCreery RL, Bergren AJ (2012) Charge transport in molecular electronic junctions: Compression of the molecular tunnel barrier in the strong coupling regime. Proc Natl Acad Sci 109:11498–11503
Sun W, Zhong J, Zhang B, Jiao K (2007) Application of cadmium sulfide nanoparticles as oligonucleotide labels for the electrochemical detection of NOS terminator gene sequences. Anal Bioanal Chem 389:2179–2184
Tombelli S, Minunni M, Luzi E, Mascini M (2005) Aptamer-based biosensors for the detection of HIV-1 Tat protein. Bioelectrochemistry 67:135–141
Üstündağ İ, Erkal A (2017) Determination of dopamine in the presence of ascorbic acid on digitonin-doped coal tar pitch carbonaceous electrode. Sens Mat 29:85–94
Vaculíková L, Plevová E, Vallová S, Koutnik I (2011) Characterization and differentiation of kaolinites from selected Czech deposits using infrared spectroscopy and differential thermal analysis. Acta Geodynamica et Geomaterialia 8(1):59–67 **[cit. 2020-07-07]**
Wei Y, Yang R, Liu J-H, Huang X-J (2013) Selective detection toward Hg (II) and Pb (II) using polypyrrole/carbonaceous nanospheres modified screen-printed electrode. Electrochim Acta 105:218–223
WHO, HIV/AIDS. https://www.who.int/news-room/fact-sheets/detail/hiv-aids. Accessed 19 Nov 2019
Yamamoto R, Kumar PK (2000) Molecular beacon aptamer fluoresces in the presence of Tat protein of HIV-1. Gene Cells 5:389–396
Yang J, Wang X, Shi H (2012) An electrochemical DNA biosensor for highly sensitive detection of phosphinothricin acetyltransferase gene sequence based on polyaniline-(mesoporous nanozirconia)/poly-tyrosine film. Sens Acta B Chem 162:178–183
Yang Y, Wang Z, Yang M, Li J, Zheng F, Shen G, Yu R (2007) Electrical detection of deoxyribonucleic acid hybridization based on carbon-nanotubes/nano zirconium dioxide/chitosan-modified electrodes. Anal Chim Acta 584:268–274
Yeter EÇ (2018) Preparation of Glass Fiber Electrode for Impedimetric DNA Analysis and its Application. Kütahya Dumlupınar University, M.Sc.
Yumak T, Kuralay F, Muti M, Sinag A, Erdem A, Abaci S (2011) Preparation and characterization of zinc oxide nanoparticles and their sensor applications for electrochemical monitoring of nucleic acid hybridization. Colloids Surf B 86:397–403
Zhang D, Peng Y, Qi H, Gao Q, Zhang C (2010) Label-free electrochemical DNA biosensor array for simultaneous detection of the HIV-1 and HIV-2 oligonucleotides incorporating different hairpin-DNA probes and redox indicator. Biosens Bioelect 25:1088–1094
Zhang Y et al (2011) An electrochemical DNA sensor based on a layers–film construction modified electrode. Analyst 136:4204–4210
Zhu N, Chang Z, He P, Fang Y (2005) Electrochemical DNA biosensors based on platinum nanoparticles combined carbon nanotubes. Anal Chim Acta 545:21–26